7TH INTERNATIONAL CONFERENCE ON CHEMICAL LOOPING 2024
BANFF, CANADA SEPT 29 TO OCT 2

7th International Conference on Chemical Looping, September 29 – October 2, 2024, Banff, Alberta, Canada

Nitrogen, Sulphur and Chlorine Balance during 80 kW_{th} Pilot Plant Operation with Bark

Fleiß Benjamin[1#], Fuchs Josef[1*], Müller Stefan[1], Hofbauer Hermann[1]

[1] *TU Wien Institute of Chemical, Environmental and Bioscience Engineering, Getreidemarkt 9, 1060 Vienna, Austria*

**Corresponding Author, josef.fuchs@tuwien.ac.at, [#]Presenting Author*

Abstract – Chemical looping combustion (CLC) of biogenic fuels offers significant potential for achieving negative CO_2 emissions by capturing CO_2 during energy production. However, ensuring high purity of captured CO_2 for compression, transport, and storage applications poses challenges, particularly due to potential impurities in biomass such as ash, phosphorus (P), sulfur (S), nitrogen (N), and chlorine (Cl). The distribution of these impurities among transport to the air reactor, binding to cyclone ash, or conversion to the gas phase, as well as their impact on reaction pathways, remains largely uncertain, varying greatly depending on the reactor system, fuel used, and oxygen carrier employed. This study focused on establishing impurity balances during pilot plant operation (80 kW_{th}) using a synthetic manganese-iron-copper oxygen carrier with bark as fuel. Through detailed analysis of gas components in the fuel reactor (FR) exhaust gas, as well as examination of bed material after the FR and the FR cyclone, nitrogen and sulfur mass balances were determined. Approximately 90 wt% of the fuel's nitrogen was converted to gaseous N_2, with the remainder mainly transported with the bed material to the air reactor (AR). Concentrations of unwanted nitrogen compounds such as NH_3, NO, and N_2O were each below 1 wt% of the fuel's nitrogen. The SO_2 concentration of the gas was low due to separation during gas analysis via water condensation and washing with rapeseeds methyl ester. A discussion of possible gas cleaning routes to meet storage requirements is based on the measured impurity levels.

1 Introduction

Chemical looping combustion (CLC) is one of the most promising carbon capture technologies for negative CO_2 emissions with biomass [1]. The separation of CO_2 during an inherent combustion step does not require any further separation processes. The oxidation of the fuel takes place separately from the combustion air and thus a pure CO_2 stream can be generated. This becomes possible by dividing the process into two reaction steps, whereby a metal-oxide (Me_yO_x), the so-called oxygen carrier (OC), is oxidized by the combustion air in a first step (1). In a second step (2), the OC delivers the oxygen and the heat necessary for combustion of the fuel (C_nH_m) and is subsequently reduced while the fuel is oxidized. The material then starts a new cycle with the oxidation reaction.

$$Me_yO_{x-1} + 1/2\ O_2 \longrightarrow Me_yO_x \quad (1)$$

$$(2n + m/2)\ Me_yO_x + C_nH_m \longrightarrow (2n + m/2)\ Me_yO_{x-1} + n\ CO_2 + m/2\ H_2O \quad (2)$$

There are two separate resulting exhaust gas streams, one ideally only consists of the combustion products CO_2 and H_2O according to reaction (2) in the so-called fuel reactor (FR) and the other one is oxygen depleted air after exiting the so-called air reactor (AR), see Figure 1. The fact that CO_2 is captured inherently with almost no energy penalty makes CLC highly efficient. In contrast to air separation or post combustion capture, CLC avoids an energy intensive gas/gas separation step to generate clean CO_2. [2]

CLC with biomass has particular potential as part of bioenergy with carbon capture and storage (BECCS) to achieve negative CO_2 emissions [3-5]. However, using solid fuels in CLC is challenging, because of the heterogeneous reactions, the ash content and the pollutant loading of the fuel. The three important levers for the improvement of the CLC technology are the selection of OC materials, the reactor design and the necessary gas cleaning to reach CO_2 purity requirements. The impurity levels in the CO_2 stream dependent on different fuel. This increases the significance for detailed investigation of reaction pathways of the impurities of the biomass, especially for critical impurities in the CO_2, like sulfur (S), nitrogen (N), and chlorine (Cl) [6, 7]. It is of great importance to design a gas cleaning route to handle these impurities and reach the purity requirements for CO_2 storage .

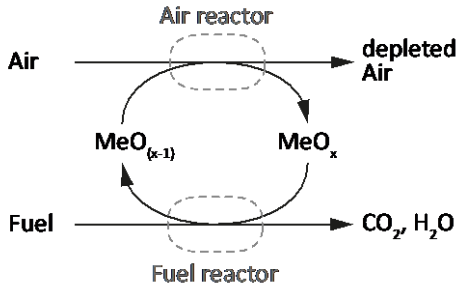

Figure 1: Scheme of the chemical looping combustion process.

This work presents the detailed impurity balances and CO_2 impurities over an 80 kW_{th} pilot plant experiments with synthetic OC and biomass. The experimental results are concluded with the proposal of a potential gas cleaning route to reach CO_2 purity requirements.

2 Methodology

2.1 80 kW_{th} pilot plant

Many pilot plants of various sizes have already been commissioned for research purposes. Although the next commercial scale up step is still pending, the dual fluidized bed (DFB) system is the preferred reactor model of most plants of larger scale. Among the plants that can be found in literature are 100 kW_{th} reactors located at Chalmers University of Technology, a 3 MW_{th} plant erected by Alstom and a 1 MW_{th} pilot plant at Darmstadt University of Technology.

Other concepts, like an 1.5 kW_{th} reactor operated by the Spanish National Research Council focus on smaller facilities. [8] The 80 kW_{th} pilot plant at TU Wien has also been planned as DFB system by Pröll and Hofbauer [9] for solid fuel CLC and Schmid et al. [10] for fluidized bed steam gasification, as shown in Figure 2. The plant consists of two fluidized beds, the AR and the FR, which are connected at the top and bottom via steam fluidized loop seals. These loop seals function as gas lock between the reactors to ensure the high CO_2 purity as well as high carbon capture rates. The AR is designed as fast fluidized bed and works as riser and serves as driving force for the OC circulation. Air can be introduced at three different levels. Through this air staging, control over the solid circulation of bed material is enabled. The entrained particles from the AR are separated from the gas by a gravity separator and transported back to the FR via the upper loop seal (ULS) [11, 12]. The FR is divided into two different zones. The lower part is designed as bubbling fluidized bed with high solids inventory to ensure proper solids residence time for char gasification. The upper part of the FR, working as a counter current column, has several internals placed along its height, reducing the free cross section of the reactor. These constrictions intensify the gas-solid contact by increasing the solid hold up. The FR is fluidized with steam, which also works as gasification agent for the solid fuels. The particles that are elutriated from the upper part of the FR are recirculated back through a gravity separator and the internal loop seal (ILS) to the bottom part of the FR.

The solids loop is closed by the lower loop seal (LLS), where the particles are transported again to the AR. For secondary solid separation of fine entrainment, both the AR and the FR are equipped with high efficiency cyclones. The fuel is fed into the lower part of the FR by on-bed feeding via a screw conveyer. Auxiliary fuel in form of fuel oil can be introduced to the AR to compensate for high heat losses caused by the large specific surface area of the pilot plant. The exhaust gas streams of the two reactors were continuously monitored with respect to O_2, CO_2, and CO (AR) as well as CO_2, CO, CH_4, H_2 and O_2 (FR) by Rosemount NGA 2000 gas analyzers (UV/IF, paramagnetic and heat conductivity). In addition, gas chromatography is used to determine N_2 and higher hydrocarbons in the FR exhaust gas.

The pilot plant is in operation since 2015 [13] and the experimental work included investigations with different fuels and different bed materials [14-17]. The first solid CLC experimental campaign with this plant was conducted and the results published 2018. [18]

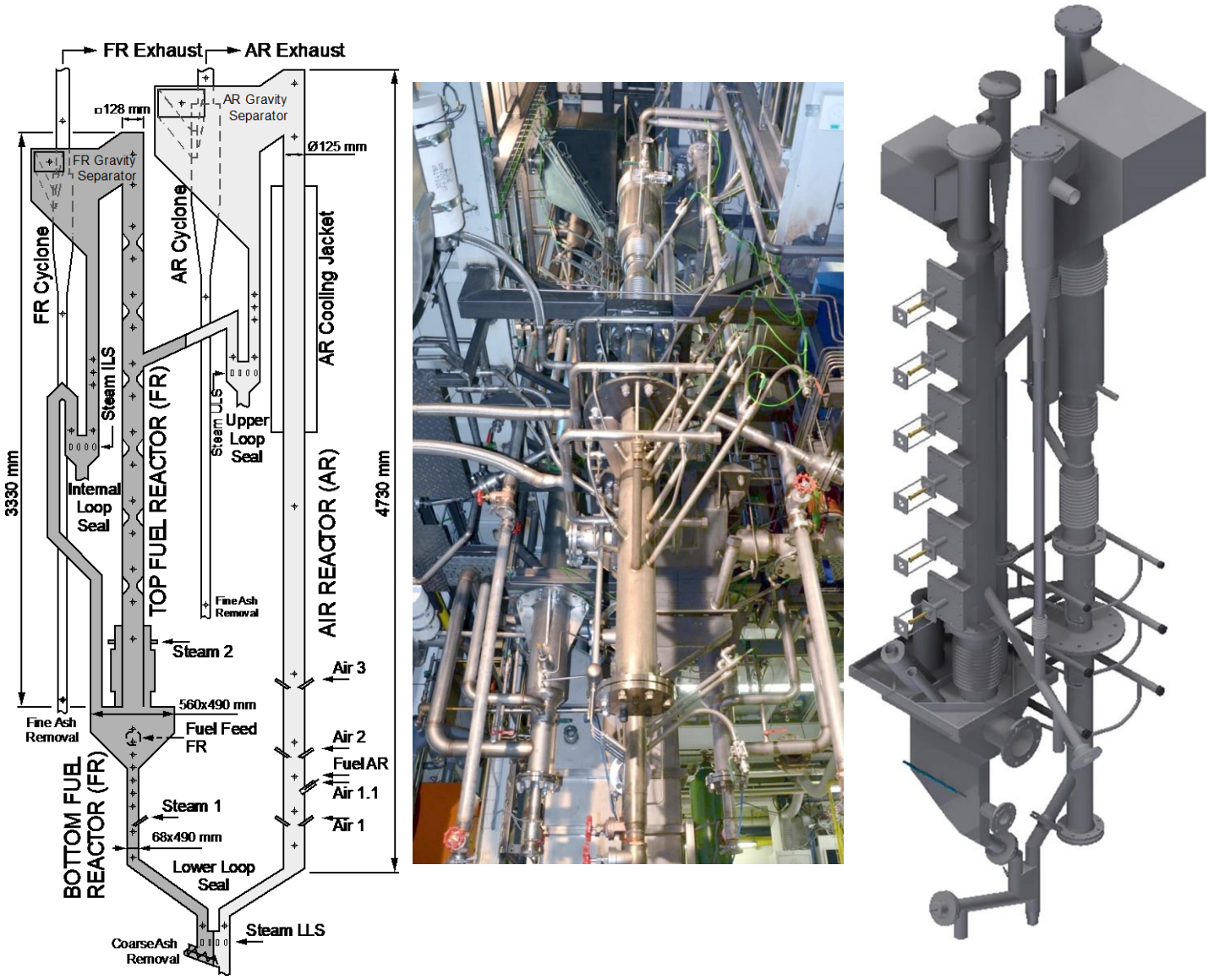

Figure 2: 80 kWth pilot plant at TU Wien, divided into FR on the left and AR on the right side.

2.2 Oxygen carrier and fuel

2.2.1 Manganese-iron-copper (MIC)

A synthetic OC, MIC (manganese-iron-copper) was used for the experimental investigations with high conversion rates and magnetic properties. The material was produced from Euro Support Advanced Materials (ESAM) with the production steps of mixing synthetic raw material, slurry formation, spray drying, calcination at 1000 °C for 24 h and sieving to a suitable particle size based on the specification of Adanez Rubio et al. [19]. The resulting composition of the material was 36% of Fe_2O_3, 33% of Mn_2O_3 and 31% CuO. The combination of the materials should provide good conversion rates and high oxygen transport, while also maintaining the chemical looping with oxygen uncoupling (CLOU) effect through the copper phase. Stability, magnetic properties and a base oxygen transport capacity are reached by the support material mixture of iron and manganese [20]. A characterization of MIC based on Fleiß et al. [21] showed consistently good properties of the material for CLC operation in the 80 kW_{th} pilot plant, seen in Figure 3. In long-term experimental investigation, the OC showed high stability in regard to reactivity and attrition but low agglomeration resistance above 950 C° [22].

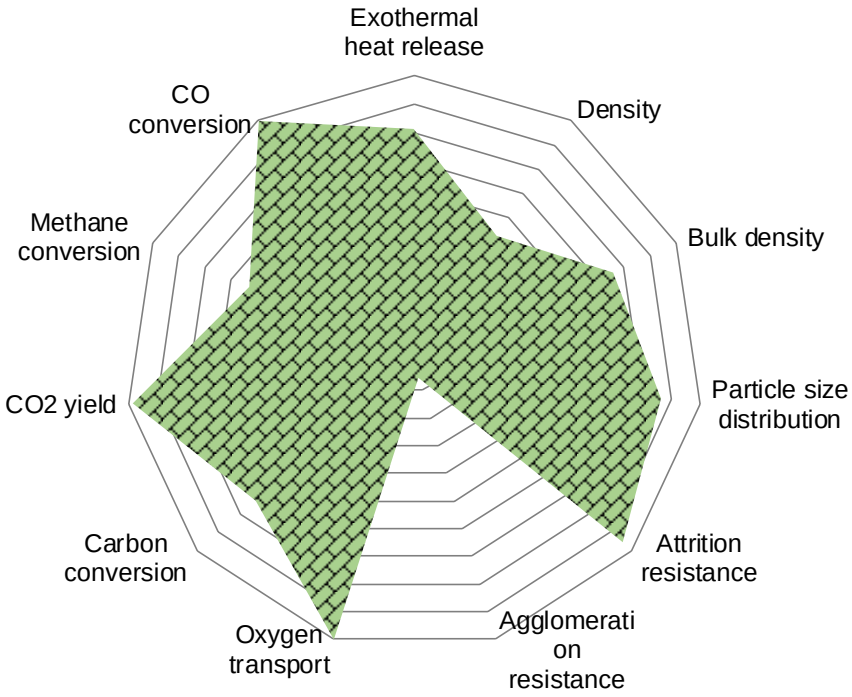

Figure 3: Laboratory characterization of MIC reaching high values and good performance.

2.2.2 Bark and sewage sludge as fuel

The fuel analyses of the different fuels used during the investigation are given in Table 1. For the experiment to investigate the reaction pathways bark was used. With the high ash content, the increased water content and some impurities the used bark pellets should simulate wood of lower fuel quality. Sewage sludge was used as high contaminated reference fuel to investigate the CO_2 purity.

Table 1: Composition of the used fuels.

		Bark	Sewage sludge
Water content	wt%	16.1	8.0
Ash	wt%(wf)	20.7	33.0
Carbon	wt%(wf)	45.03	34.0
Hydrogen	wt%(wf)	3.4	5.0
Oxygen	wt%(wf)	rest	rest
Nitrogen	wt%(wf)	0.7	5.0
Sulphur	wt%(wf)	0,06	1.0
Chlorine	wt%(wf)	0.01	0.1
Volatiles	wt%(waf)	69,9	-
LHV (dry)	kJ/kg(wf)	20300	-

2.3 Measurements and evaluation

To deduct the fate of the fuel impurities N, S and Cl, it must be specified to which form the fuel impurities convert during the operation. Linderholm et al. [23] gives an overview of the different S and N phases of CLC operation with coal and ilmenite. Sulfur converts mainly to SO_2 and a small fraction of H_2S in the FR. Some of the fuel sulfur is also bound by the OC and the ash while a part may be transported with fuel char to the AR. The nitrogen which is converted to the gas phase is distributed to N_2, NH_3, NO and a minor fraction of HCN (below 1 wt%). Chlorine is converted to gaseous HCl while a main fraction is bound by different phases of the bed material and ash like KCl, $CaCl_2$, CuCl and $(CuCl)_3$ [24]. Also, most of the HCl is condensing already at high temperatures and is therefore hard to detect. The measurement methods of the different phases are given in Table 2.

Table 2: Planned measurement setup of the different impurity phases. (Rosemount= Rosemount NGA 2000, GC= Perkin Elmer Arnel Clarus® 500 gas chromatographic, Gas bag + GC = transport gas bag to Perkin Elmer Arnel Clarus® 500 with a flame photometric detector and a thermal conductivity detector, VDI 3878=wet chemical analysis with H_2SO_4,

Sulfur	Method	Nitrogen	Method	Chlorine	Method
SO_2	Rosemount	N_2	GC	HCl	Absorption
H_2S	Gas bag + GC	NO	Rosemount		
COS	Gas bag + GC	N_2O	Rosemount		
C_4H_4S	Gas bag + GC	NO_2	Rosemount		
		NH_3	VDI 3878		
		HCN	-		
OC/char to AR		CHNS analysis + XRF			
Cyclone		CHNS analysis + XRF			

Mass and energy balance modeling and data evaluation were performed using the simulation software IPSEpro by Simtech Simulation Technology. It is a steady-state, equation-oriented software for the simulation of power and chemical plants and can be used for process evaluation, detail engineering and design, monitoring and optimization of existing plants as well as for statistical validation of measurement data. The big advantage of IPSEpro is its modular structure giving the user full control over the whole simulation process. This includes full knowledge about the used models and property data without limitations in expanding existing models and libraries. A detailed description of the experimental setup and procedure is given by Fleiß et al. [25]. By default, in the AR exhaust gas CO_2, CO and O_2 are measured. In the FR exhaust gas, a Perkin Elmer Arnel Clarus® 500 gas chromatographic measurement is carried out in addition to a continuous measurement of the concentration of gases. The gases measured include O_2, CO_2, CO, CH_4, H_2, N_2, C_2H_2, C_2H_4 and C_2H_5. [22, 25, 26]

3 Results and Discussion

3.1 N-balance of MIC and bark

Figure 4 illustrates the nitrogen mass balance and its components using a Sankey diagram. The width of each arrow represents the mass of nitrogen converted into different phases. The 59.3 g/h of nitrogen introduced via the bark pellets are separated into different streams through reactions in the FR. The majority of the nitrogen is converted to gaseous nitrogen (N_2), while gas impurities like NO, N_2O, NH_3, and NO_2 are kept at 1.1 wt% or below. Some of the nitrogen remains in the char discharged from the FR, ends up in the cyclone and transported to the AR.

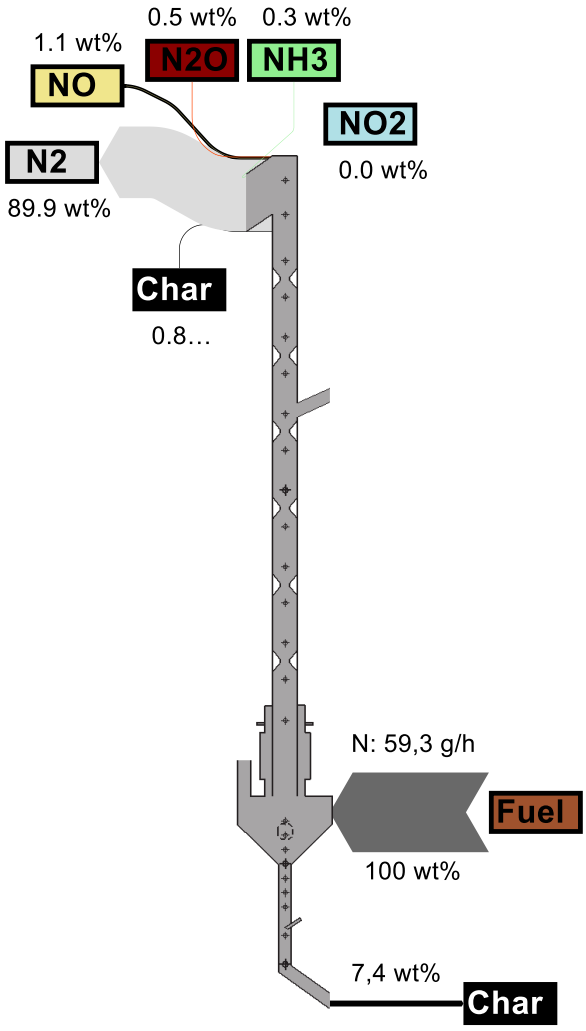

Figure 4: Nitrogen balance in form of Sankey diagram over the FR reactor.

Additionally, 280 g/h of nitrogen is used for flushing pressure measurements and the fuel bunkers. This nitrogen flushing is not depicted in the figure since no conversion is expected to occur during operation. Despite validation through simulation, the high amount of nitrogen in the char of the lower loop seal (LLS) involves some uncertainties. It's possible that char accumulates in the LLS, and the solid sample does not represent a selective mixture of the material transported to the air reactor (AR). This could be due to the low density of char, which causes it to float to the surface of the fluidized bed and not be transported to the other side of the loop seal, leading to char accumulation in the LLS.

The CHNS analysis indicates a char concentration of 0.21 wt% in the LLS sample, which is reduced to 0.03 wt% after validation with IPSEpro to fulfil the mass balance due to the high uncertainty of the measurement method. However, if there is less nitrogen transport to the AR via the LLS, the main adjustment in the calculation would be shifting from char to N_2 in the gas phase, given the decreased certainty influenced by nitrogen flushing. This implies that the actual gas impurities, NO, N_2O, NH_3, and NO_2, would remain low. Considering the gas measurements from the AR and the low amount of NO_X, it is concluded that over 98 wt% of fuel nitrogen is

converted to non-critical species. Therefore, it is likely feasible to use fuel with low nitrogen concentration without increasing the gas cleaning effort for CO_2.

3.2 S-balance of MIC with bark

Figure 5 illustrates the sulfur mass balance in the same way as discussed for nitrogen. A significant proportion of the sulfur remains in the char and is transported via the lower loop seal (LLS) to the air reactor (AR). In the sulfur balance, the uncertainty of the char concentration in the LLS coincides with the uncertainty of SO_2 measurement due to absorption in the condensed water. Despite selecting a high range of standard deviation, validation calculations indicated high sulfur transport via the loop seal based on the measurements. The affinity of sulfur to ash, carbon char, and oxygen carriers (OC) could explain the significant distribution between gas and char sulfur. Additionally, the char discharged to the cyclone shows a high concentration of sulfur.

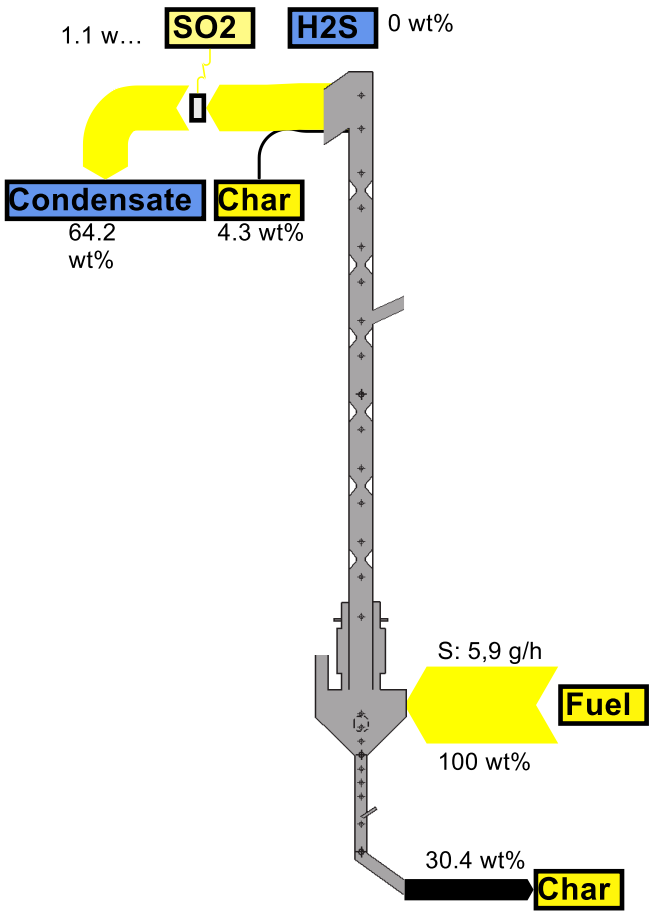

Figure 5: Sulfur balance in form of Sankey diagram over the FR reactor.

As no SO_2 was detected in the AR exhaust gas, the ultimate fate of the sulfur is not entirely clear. It is expected that the majority of the sulfur (64.2 wt%) would be found in the scrubbing liquid of the gas measurement system, with a small portion adsorbed on the ash and OC. No other sulfur-containing gas components, such as H_2S, COS, or C_4H_4S, were measured, which is advantageous for gas cleaning since SO_2 purification is a well-established process in flue gas cleaning.

3.3 Cl-balance and ash of MIC with bark

During the experiment, no gas species of Cl, such as HCl, were measured in the FR exhaust gas. The XRD analyses of the solid samples from the cyclone and LLS show also no signs of concentrations of chlorine in the solid sample, as seen in Table 3. This could be a result of the low chlorine concentration of the fuel. In general, chlorine has a high tendency to stay at surfaces like ash, OC, or char particles, as well as reactor or heat exchanger linings. To evaluate the fate of chlorine more precisely in the different gas phases, a high chlorine concentration in the fuel would have been required. However, proving the existence of different chlorine gas phases is difficult due to the high condensing temperature. The utilization of synthetic OC with chlorine-containing fuel is not optimal due to deactivation and the loss of OC [24].

The concentration of the ash particles in the cyclone was higher than in the LLS. However, due to the high solid circulation rate, the total amount of ash remaining in the bed material was higher than that in the discharged material. This suggests an accumulation of ash in the bed material and could prove to be critical in long-term operation. In this case, a bed material exchange by separation of OC would be necessary to prevent the overloading of ash in the reactor. An interesting factor is the increased concentration of CuO and decreased concentration of Fe_2O_3 of the cyclone solid sample, which suggests different stabilities of the OC phases and primarily low concentration of Fe in fines. However, the discrepancy between the original composition of MIC with a high concentration of CuO of over 30 wt% and the solid samples could not be fully explained by this factor. A part of the ultra-fines of copper could have bypassed the cyclone and ended up in the bag filter of the pilot plant. A high concentration of CaO in the cyclone sample is also noticeable. This could mean that CaO as part of the fuel ash tends to be transported to the cyclone due to lower particle stability and lower density.

Table 3: XRF-analyses of relevant elements of solid samples from LLS and cyclone during operation with MIC and bark pellets.

wt%	LLS	Cyclone	Bark ash
CuO	13.06	15.37	0.1
Fe_2O_3	41.21	24.68	3.9
MnO	37.77	37.26	0.8
Cr_2O_3	0.09	0.1	0.1
TiO_2	0.6	0.27	0.8
CaO	3.09	15.1	16.6
K_2O	0.54	0.82	8.7
Cl	n.a.	n.a.	0.2
SO_3	0.29	0.28	0.5
P_2O_5	0.42	1.15	0.7
SiO_2	1.52	2.04	50.1
Al_2O_3	0.25	1.17	11.6
MgO	0.94	1.43	2
Na_2O	0.12	0.2	2.1
Ash est.	7.96	22.69	

3.4 C-balance of MIC with bark

Figure 6 illustrates the carbon mass balance. The 4372 g/h of carbon introduced via the bark pellets are separated into different streams through reactions in the FR. Most of the carbon is converted to CO_2, while unburnt gas species like CH_4, C_3H_8, and CO are measured below 1 wt%. Other hydrocarbons such as C_2H_2, C_2H_4, and C_2H_6 were below the detection range of the gas chromatograph (GC). Less than 5 wt% of carbon is transported via the lower loop seal (LLS) to the air reactor (AR). This value is double-validated by the CO_2 measurement in the AR exhaust gas, where the gas measurement estimates the carbon loss to the AR to be lower than the CHNS analysis of the LLS solid sample.

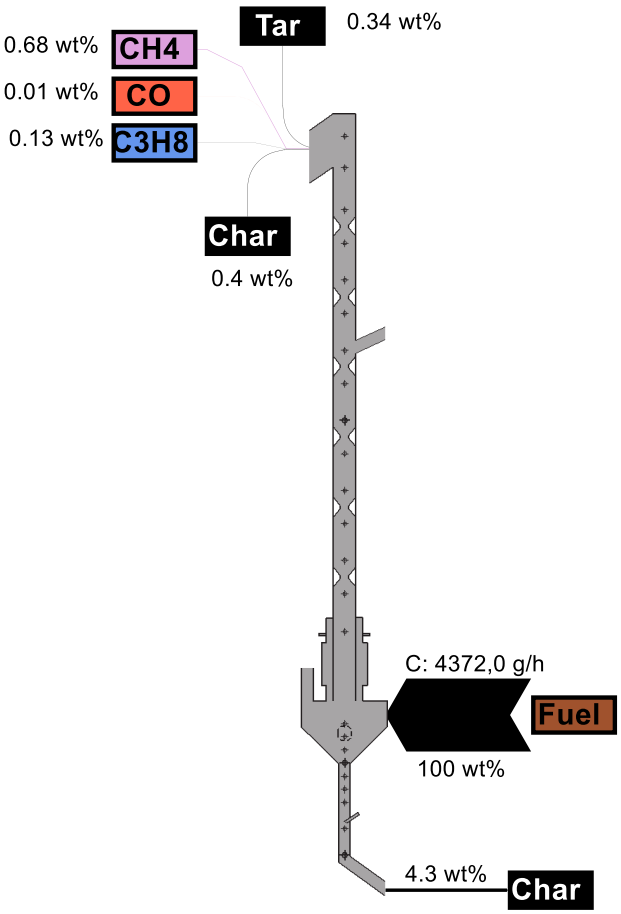

Figure 6: Carbon balance in form of Sankey diagram over the FR reactor.

A smaller fraction of carbon is lost to the cyclone as char, and low concentrations of tar and flue coke are measured in the CO_2 stream. Overall, a CO_2 yield of 94.2% was achieved. This yield could potentially be increased with more favourable process conditions – such as higher temperature, increased solid circulation rate, and higher oxidation state reached in the AR via increased airflow and/or residence time.

3.5 Gas purity and CO_2 requirements

The measured CO_2 impurities of the experiments with MIC combusting bark and sewage sludge are compared to purity requirements of different sources and applications, as seen in Table 4. When considering the purity requirements in comparison to MIC with bark, two critical components become apparent: the oxygen generated through the release from CLOU OC and the NO_X, which is oxidized from fuel nitrogen. For many applications, these components must be purified. The nitrogen concentration would be lower since the experiment was conducted with nitrogen flushing and should therefore meet the requirements. H_2, CO, and NH_3 narrowly miss some of the requirements. These can likely be achieved through optimized operating conditions. The SO_X concentration meets most of the requirements but can probably be easily purified by adding limestone to the bed material or lime milk to the condensing step. In comparison, contaminations with sewage sludge are more severe, and most purity requirements are far exceeded. Excessive gas cleaning would be necessary to meet the purity criteria, incurring additional costs. Therefore, it is critical to question whether CLC is a suitable technology for capturing CO_2 from sewage sludge or other heavily contaminated fuels. However, the required purity can certainly be achieved with appropriate gas-cleaning processes. Additionally, it is noteworthy that the literature varies significantly in terms of purity, and there are still no official guidelines for CO_2 purity for compression, transport, and storage.

Table 4: CO_2 impurities of the experiments compared to literature requirements for different CO_2 storage applications. [27]

Component	Unit	Lyngfelt et al. [7]	Murugan et al. [28]	DNV-GL-RP F104 [29]	Netl [30]	Dynamis [31]	Porthos [32]	MIC bark	MIC sewage sludge
CH_4	vol%	-	4	2	4	2	1	0.69	1.71
N_2	vol%	-	4	-	4	-	2.4	1.54	7.77
H_2	vol%	0.005	1	-	4	4	0.75	0.21	0.30
O_2	ppm	10	10	10	10	40000	40	290	500
CO	ppm	100	20	400	35	2000	750	123	701
SO_X	ppm	10	0.5	100	100		20	5	477
NO_X	ppm	10	0.5	100	100		5	159	1390
H_2S	ppm	9	5	100	100	200	5	0	0
NH_3	ppm	10	25		50		5	41	253
HCl	ppm	-	1	-	-	-	-	0	Not measured

3.6 Suggested gas cleaning route

Based on the experimental results with the synthetic OC, the main critical impurities are NO_X and O_2. It is probably possible to reduce the other impurities like H_2, CO and NH_3 by adaptions of the operational setup, e.g., increasing the height of upper FR and therefore the residence time of the gas. A possible gas cleaning route for CO_2 from CLC with synthetic OC is shown in Figure 7. After CLC process a cooling should take place to extract usable heat. After that, an electrostatic precipitator or bag filter enables the separation of fines and ash. The selection of the particle separation unit depends on temperature levels but also on airtight operation to reduce ingress of air. During the first condensation step, extra heat, condensed water and SO_2 can be extracted. For high SO_2 concentration the adding of limewater to the condensation would be necessary. Else, the SO_2 would act as a catalyst poison in the Selective Catalytic Reduction step. At around 300 °C, the NO_X reacts with O_2 and NH_3 over a catalytic material (vanadium, molybdenum or tungsten) to N_2 and water. To reduce the O_2 concentration an addition of H_2 may be necessary to catalytically convert O_2 and reduce probably other unwanted gases like CO, CH_4 and NH_3. Depending on compression process, the H_2O concentration has to be lowered in a second condensation step. Other compression processes include the water separation in the liquefaction step of the CO_2. The suggested gas cleaning route is partly based on Lyngfelt et al. [7, 33] with natural ores as OC. The actual purification and provision of CO_2 from CLC for storage has not yet been tested. There are also some uncertainties regarding the final CO_2 purity levels required for compression, transport, and storage.

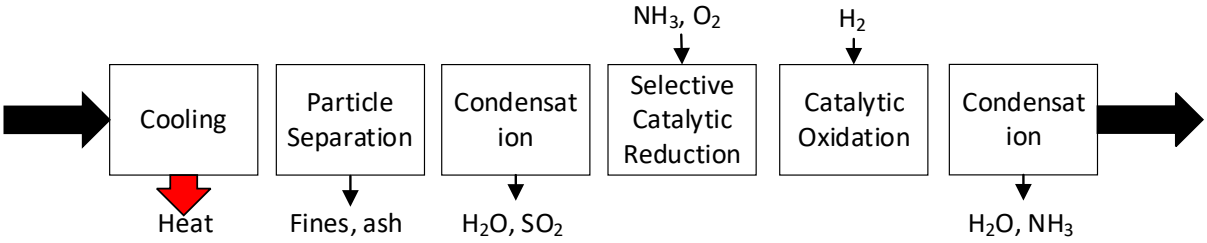

Figure 7: Suggested gas cleaning for CO_2 purification of CLC exhaust gas from operation with synthetic OC for CO_2 storage.

4 Conclusion

In this work the efficient chemical looping combustion technology for negative CO_2 emissions from biomass was investigated regarding the CO_2 purities and reaction pathways from fuel impurities with a synthetic oxygen carrier. CO_2 purities over 97% were reached where the main impurities were based on nitrogen in the form N_2 and low amounts of the critical gases NO and N_2O. Only low amounts of SO_2 were measured because most of it was separated during a condensation step. Based on the measured impurities, the main additional gas cleaning effort will come with O_2 and the NO_X concentration. Finally, a gas cleaning route was suggested in order to reach the needed CO_2 purities limits for compression, transport and storage.

References

[1] Coppola A., Scala F. (2021) Chemical Looping for Combustion of Solid Biomass: A Review, *Energy & Fuels*. **35(23)**: p. 19248-19265.

[2] Adánez J., Abad A. (2019) Chemical-looping combustion: Status and research needs, *Proceedings of the Combustion Institute*. **37(4)**: p. 4303-4317.

[3] Pikkarainen T., Hiltunen I., Teir S. (2016) Piloting of bio-CLC for BECCS, in *4th International Conference on Chemical Looping*: Nanjing, China.

[4] Lindroos T.J., Rydén M., Langørgen Ø., Pursiheimo E., Pikkarainen T. (2019) Robust decision making analysis of BECCS (bio-CLC) in a district heating and cooling grid, *Sustainable Energy Technologies and Assessments*. **34**: p. 157-172.

[5] Emenike O., Michailos S., Finney K.N., Hughes K.J., Ingham D., Pourkashanian M. (2020) Initial techno-economic screening of BECCS technologies in power generation for a range of biomass feedstock, *Sustainable Energy Technologies and Assessments*. **40**.

[6] Lyngfelt A., Andersson K., Pettersson L.R. (2022) Design of circulation system and downstream gas treatment of a full-scale boiler for Chemical-Looping Combustion, *SSRN Electronic Journal*.

[7] Lyngfelt A., Petersson L., Andersson K. (Year) Downstream Gas Treatment to Attain Storage Quality of CO_2 from Chemical-Looping Combustion. in *6th International Conference on Chemical Looping*. Zaragoza, Spain.

[8] Abad A., Adánez-Rubio I., Gayán P., García-Labiano F., de Diego L.F., Adánez J. (2012) Demonstration of chemical-looping with oxygen uncoupling (CLOU) process in a 1.5kWth continuously operating unit using a Cu-based oxygen-carrier, *International Journal of Greenhouse Gas Control*. **6**: p. 189-200.

[9] Pröll T., Hofbauer H. (2010) A dual fluidized bed system for chemical looping combustion of solid fuels, *Proceedings of the AIChE Annual Meeting 2010 Salt Lake City, USA*.

[10] Schmid J., Pröll T., Pfeifer C., Hofbauer H. (2011) Improvement of gas-solid interaction in dual circulating fluidized bed systems, in *Proceedings of the 9th Conference on Industrial Furnances and Boilers (INFUB-9)* Estoril, Portugal.

[11] Penthor S., Stollhof M., Pröll T., Hofbauer H. (2016) Detailed fluid dynamic investigations of a novel fuel reactor concept for chemical looping combustion of solid fuels, *Powder Technology*. **287**: p. 61-69.

[12] Pröll T., Kolbitsch P., Bolhàr-Nordenkampf J., Hofbauer H. (2009) A novel dual circulating fluidized bed system for chemical looping processes, *AIChE Journal*. **55(12)**: p. 3255-3266.

[13] Schmid J.C., Müller S., Hofbauer H. (2016) First scientific results with the novel dual fluidized bed gasification test facility at TU Wien, in *24th European Biomass Conference and Exhibition (EUBCE), ETA-Florence Renewable Energies*: Amsterdam, The Netherlands. **p. 842-846**.

[14] Benedikt F., Fuchs J., Schmid J.C., Müller S., Hofbauer H. (2017) Advanced dual fluidized bed steam gasification of wood and lignite with calcite as bed material, *Korean Journal of Chemical Engineering*. **34(9)**: p. 2548-2558.

[15] Fuchs J., Schmid J., Müller S., Hofbauer H. (2018) Sorption Enhanced Reforming: Transport Characteristics of CO_2 and Char, in *11th International Conference on Sustainable Energy & Environmental Protection*: University of the West of Scotland, Paisley, United Kingdom.

[16] Mauerhofer A.M., Benedikt F., Schmid J.C., Fuchs J., Müller S., Hofbauer H. (2018) Influence of different bed material mixtures on dual fluidized bed steam gasification, *Energy*. **157**: p. 957-968.

[17] Müller S., Fuchs J., Schmid J.C., Benedikt F., Hofbauer H. (2017) Experimental development of sorption enhanced reforming by the use of an advanced gasification test plant, *International Journal of Hydrogen Energy*. **42(50)**: p. 29694-29707.

[18] Penthor S., Fuchs J., Benedikt F., Schmid J., Mauerhofer A., Mayer K., Hofbauer H. (2018) First results from an 80 kW dual fluidized bed pilot unit for solid fuels at TU Wien, in *5th International Conference on Chemical Looping*: Park City, Utah, USA.

[19] Adánez-Rubio I., Bautista H., Izquierdo M.T., Gayán P., Abad A., Adánez J. (2021) Development of a magnetic Cu-based oxygen carrier for the chemical looping with oxygen uncoupling (CLOU) process, *Fuel Processing Technology*. **218**.

[20] Abad A., Pérez-Vega R., Izquierdo M.T., Gayán P., García-Labiano F., de Diego L.F., Adánez J. (2021) Novel Magnetic Manganese-Iron Materials for Separation of Solids Used in High-Temperature Processes: Application to Oxygen Carriers for Chemical Looping Combustion, *SSRN Electronic Journal*.

[21] Fleiß B., Penthor S., Müller S., Hofbauer H., Fuchs J. (2022) Holistic assessment of oxygen carriers for chemical looping combustion based on laboratory experiments and validation in 80 kW pilot plant, *Fuel Processing Technology*. **231**.

[22] Fleiß B., Priscak J., Hammerschmid M., Fuchs J., Müller S., Hofbauer H. (2024) CO_2 capture costs of chemical looping combustion of biomass: A comparison of natural and synthetic oxygen carrier, *Journal of Energy Chemistry*.

[23] Linderholm C., Knutsson P., Schmitz M., Markström P., Lyngfelt A. (2014) Material balances of carbon, sulfur, nitrogen and ilmenite in a 100kW CLC reactor system, *International Journal of Greenhouse Gas Control*. **27**: p. 188-202.

[24] Huang H., Ma J., Zhao H., Zheng C. (2023) Behavior of coal-chlorine in chemical looping combustion, *Proceedings of the Combustion Institute*. **39(4)**: p. 4437-4446.

[25] Fleiß B., Priscak J., Fuchs J., Müller S., Hofbauer H. (2023) Synthetic oxygen carrier C28 compared to natural ores for chemical looping combustion with solid fuels in 80 kW_{th} pilot plant experiments, *Fuel*. **334**.

[26] Fleiß B., Bartik A., Priscak J., Benedikt F., Fuchs J., Müller S., Hofbauer H. (2023) Experimental demonstration of 80 kW_{th} chemical looping combustion of biogenic feedstock coupled with direct CO_2 utilization by exhaust gas methanation, *Biomass Conversion and Biorefinery*.

[27] Fleiß B. (2024) Investigation of Chemical Looping Combustion in Fluidized Beds as Bioenergy Carbon Capture and Storage Technology, in *Institute of Chemical, Environmental and Bioscience Engineering*, TU Wien: Vienna.

[28] Murugan A., Brown R.J.C., Wilmot R., Hussain D., Bartlett S., Brewer P.J., Worton D.R., Bacquart T., Gardiner T., Robinson R.A., Finlayson A.J. (2020) Performing Quality Assurance of Carbon Dioxide for Carbon Capture and Storage, *C*. **6(4)**.

[29] DNV-RP-F104 (2017) Design and operation of carbon dioxide pipelines, E. 2021-02, Editor.

[30] Shirley P., Myles P. (2019) Quality Guidelines for Energy System Studies: CO_2 Impurity Design Parameters, National Energy Technology Laboratory (NETL): Pittsburgh.

[31] de Visser E., Hendriks C., Barrio M., Mølnvik M.J., de Koeijer G., Liljemark S., Le Gallo Y. (2008) Dynamis CO2 quality recommendations, *International Journal of Greenhouse Gas Control*. **2(4)**: p. 478-484.

[32] Porthos (2021) CO_2 specifications.

[33] Lyngfelt A., Pallarès D., Linderholm C., Lind F., Thunman H., Leckner B. (2022) Achieving Adequate Circulation in Chemical Looping Combustion—Design Proposal for a 200 MW_{th} Chemical Looping Combustion Circulating Fluidized Bed Boiler, *Energy & Fuels*. **36(17)**: p. 9588-9615.